Volume reflection and volume capture of ultrarelativistic particles in bent single crystals

S. Bellucci,[1] Yu. A. Chesnokov,[2] V. A. Maisheev,[2] and I. A. Yazynin[2]
[1]*INFN-Laboratori Nazionali di Frascati, Via Enrico Fermi 40, 00044 Frascati, Italy*
[2]*Institute for High Energy Physics in National Research Centre "Kurchatov Institute," 142281 Protvino, Russia*
(Received 24 June 2015; published 30 November 2015)

The paper is devoted to the study of volume reflection and volume capture of high energy particles moving in planar fields of bent single crystals. The influence of volume capture on the process of volume reflection was considered analytically. Relations describing various distributions of particles involved in the process, the probability of volume capture and the behavior of channeling and dechanneling fractions of a beam were obtained. Results of the study will be useful in the realization of multicrystal devices for collimation and extraction of beams on modern and future accelerators.

DOI: 10.1103/PhysRevSTAB.18.114701 PACS numbers: 61.85.+p, 41.60.−m, 78.70.−g, 41.20.Jb

I. INTRODUCTION

Volume reflection of charged particles in single crystals represents the coherent scattering of these particles by planar or axial electric fields of bent crystallographic structures. For the first time, this effect was predicted in Ref. [1] on the basis of Monte Carlo calculations. Recently in Ref. [2] an analytical description of volume reflection of ultrarelativistic particles was considered. After this, other models of the process were published [3–6]. Besides, this process was observed and investigated in a number of experiments [7–9].

Results of the study of volume reflection are of interest to a series of important applications for accelerator technics (such as beam collimation, extraction and others). For the working out of these applications it is assumed the use of a volume reflection process repeated many times (in special crystal structures). One can expect that, due to the high efficiency of the process, the total efficiency of crystal devices will be also high enough.

The main process which influences the efficiency of volume reflection is volume capture [10,11]: when moving in bent single crystals, particles may (due to multiple scattering on atoms) be captured in a channeling regime. The analytical description of volume reflection (see [2]) gives good predictions for many characteristics of the process, but volume capture was not considered in this theory.

This paper is devoted to the complete analytical consideration of volume reflection, including the influence of volume capture on the process. Main results of Ref. [2] remain valid but their updating is required. No doubt that Monte Carlo simulations give detailed information about the process at some specific initial conditions. However, an analytical description allows one to make the observation of the problem as a whole.

The calculations performed in accordance with relations of Ref. [2] show that the accuracy of the analytical calculations of parameters such as the mean and mean square angles at volume reflection is in the same agreement with the experiment as the results of Monte Carlo simulations [12,13].

Besides, in Ref. [2] it is shown how to use generalized parameters for the description of the process. Because of this, one can obtain a set of results from one calculated result. It is important for the emulation of the process, when the experimental results are known at some conditions (for example, for one energy of the beam) and these results should be used at different conditions (e.g., for another energy).

The main electrodynamic processes (such as the bremsstrahlung of electrons and positrons or the photoproduction of $e^{\pm}$-pairs) in bent single crystals have peculiarities and were considered in particular, in the paper [14]

The paper is organized as follows. First, we give the mathematical description of the unperturbed characteristics of the volume reflection process and make a comparison with measurements. After that we describe our method for the study of diffusion processes in bent single crystals. Then, based on this method, we find the probability of volume capture and energy distribution underbarrier particles. After that we investigate the behavior of the channeling fraction at its propagation in a single crystal. As a result we get the analytical relations for distribution functions of particles.

In the last part of the paper we illustrate the obtained relations by numerical calculations and then we discuss and summarize the results presented in the paper.

II. UNPERTURBED CHARACTERISTICS OF VOLUME REFLECTION

A. Main relations for the volume reflection description

Volume reflection of charged particles in single crystals represents the coherent scattering of these particles by planar or axial fields of bent crystallographic structures. Here we will consider only the planar case.

Our analytical description of the volume reflection is based on well-known equations for the particle motion in bent planar fields of single crystals. In particular the following equation is valid for such a motion:

$$E_0\beta^2 v_x^2/(2c^2) + U(x) + E_0\beta^2 x/R = E, \qquad (1)$$

where E_0, E, and β are the total and transverse energies of the particle and its velocity divided by the velocity of light c, $U(x)$ is the periodic planar potential in the straight single crystal as a function of the coordinate, R is the radius of bending, x is the transverse coordinate.

Really Eq. (1) describes the one-dimensional particle motion in the effective potential $U_e(x) = U(x) + E_0\beta^2 x/R$. Figure 1 illustrates the particle motion in this potential. One can see that the particle moving in the direction of increasing of the effective potential undergoes reflection. The trajectory 2 illustrates the volume capture process.

On the first step of our approach an unperturbed (by multiple scattering on atoms) motion of charged particles is considered. On the second step we introduce multiple scattering and get the complete characteristics of the process.

In accordance with [2] the angle of volume reflection is equal to:

$$\alpha(E) = \frac{2c}{R}\int_{x_0}^{x_c}\left[\frac{1}{\sqrt{\frac{2c^2}{E_0\beta^2}\left[E - U(x) - E_0\beta^2 x/R\right]}} - \frac{1}{\sqrt{\frac{2c^2}{E_0\beta^2}\left[E - U(x_c) - E_0\beta^2 x/R\right]}}\right]dx, \qquad (2)$$

where the critical point x_c is the solution of the equation $E - U(x_c) - E_0\beta^2 x_c/R = 0$; x_0 is the initial coordinate of a particle and satisfies the equation $E_0\beta^2\theta^2/2 + U(x_0) + E_0\beta^2 x_0/R = E$ (θ is the entrance angle in a single crystal). Equation (2) is written for the symmetric case of particle passage through a single crystal. In this case $|x_0 - x_c| \approx |x_e - x_0| \approx l_0^2/(8R)$, where l_0 is the thickness of a single crystal and x_e is the exit coordinate (in the common case one integral $2\int_{x_0}^{x_c}$ in Eq. (2) should be changed on sum $\int_{x_0}^{x_c} + \int_{x_c}^{x_e}$). Equation (2) was obtained under the assumption that multiple scattering is turned off but it is valid also for the case when multiple scattering takes place (see below).

One can see that Eq. (2) describes the volume reflection angle as a function of the parameter E. It is easy to understand [due to the periodicity of $U(x)$] that the function $\alpha(E)$ is a periodic function with the period $\delta E = E_0\beta^2 d/R$. One can find the following expression for the distribution function of scattered particles over the volume reflection angle

$$\left\langle \frac{dN}{d\alpha}(\alpha) \right\rangle = \frac{1}{\delta E}\sum_j \left|\frac{d\alpha}{dE}\right|^{-1} \qquad (3)$$

where the sum over j means that the sum should be taken over every domain of the function single-valuedness and the derivative $d\alpha/dE$ should be calculated for values E_j which satisfy the equation $\alpha(E_j) = \hat{\alpha}$ in which $\hat{\alpha}$ is the current value of the volume reflection angle.

In Ref. [2] it is shown that the mean and mean square angles of volume reflection can be found from the equations

$$\langle \alpha_{vr} \rangle = \frac{1}{\delta E}\int_E^{E+\delta E} \alpha(E)dE, \qquad (4)$$

$$\sigma_{vr}^2 = \frac{1}{\delta E}\int_E^{E+\delta E} (\alpha(E) - \langle\alpha\rangle)^2 dE \qquad (5)$$

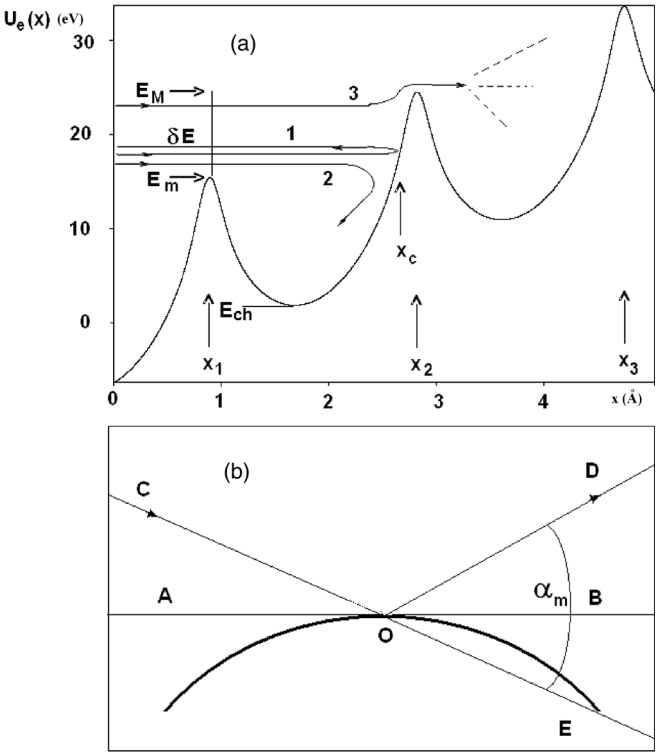

FIG. 1. Scheme of volume reflection and volume capture processes: (a) the effective potential of bent crystallographic planes, x is the transverse coordinate. E_M and E_m are the transverse energies corresponding to neighboring local maxima of the potential; E_{ch} is one of the transverse energies corresponding to a local minimum of potential; x_1, x_2, x_3 are the transverse coordinates of the local maxima; the curves 1,2,3 reflect the different possibilities for moving particles. x_c is the critical coordinate for volume reflected particles; (b) geometric relations of the process. For additional information, see the text.

Here we used the result obtained in the paper [2]: $\langle \frac{dN}{dE}(E) \rangle = 1/\delta E$, where N is the number of charged particles (normalized on unit) per period of the transverse energy. Equations (2)–(5) were written for the unperturbed (by multiple scattering) case. The exit distribution of particles (from a single crystal) which takes into account multiple scattering reads

$$\left\langle \frac{dN}{d\alpha}(\alpha) \right\rangle_{\text{exit}} = \int_{-\infty}^{\infty} \rho_{ms}(\varphi, \sigma_{ms}) \left\langle \frac{dN}{d\alpha}(\alpha - \varphi) \right\rangle d\varphi, \quad (6)$$

where $\rho_{ms}(\varphi, \sigma_{ms})$ is the normal distribution describing multiple scattering and the mean square angle σ_{ms} corresponds to the thickness of a crystal. It is easy to generalize Eq. (6) for the case of a beam with a valuable angle divergence [with the distribution $\rho_b(\alpha)$)].

For the mean angle of volume reflection of the resulting distribution $\rho_R(\alpha)$ we get

$$\langle \alpha_R \rangle = \langle \alpha_b \rangle + \langle \alpha_{ms} \rangle + \langle \alpha_{vr} \rangle, \quad (7)$$

where $\langle \alpha_R \rangle, \langle \alpha_b \rangle, \langle \alpha_{ms} \rangle$, and $\langle \alpha_{vr} \rangle$ are the mean values of $\rho_R, \rho_b, \rho_{ms}$, and $\langle \frac{dN}{d\alpha}(\alpha) \rangle$ distributions, correspondingly. They are calculated in the coordinate system where the zero angle coincides with the entrance angle θ. Note that $\langle \alpha_{ms} \rangle = 0$ for a normal distribution. For the dispersion of the resulting distribution we get the relation:

$$\sigma_R^2 = \sigma_b^2 + \sigma_{ms}^2 + \sigma_{vr}^2, \quad (8)$$

where $\sigma^2 = \int_{-\infty}^{\infty} (\alpha - \langle \alpha \rangle)^2 \rho(\alpha) d\alpha$.

The characteristics ($\langle \alpha_{vr} \rangle$ and σ_{vr}) obtained here can be considered as unperturbed ones. In our case it means that we do not consider such a process as volume capture when moving particles lose their transverse energy and are captured in the channeling regime. Below we consider in detail the volume capture and its influence on volume reflection.

B. Comparison of the theory with experimental data

In late years the study of the volume reflection process was performed both experimentally and theoretically. We think that it is useful to compare the theoretical consideration presented above with measurements. Most of the measurements were carried out with the (110) and (111) planes of the silicon single crystals. In these experiments such important characteristics as the mean angle of the volume reflection and its mean square were obtained. The method of finding these characteristics from results of measurements was described in [15]. It is easy to see that long tails of experimental distributions were ignored in the analysis. It means that the obtained quantities of the above pointed characteristics correspond to their unperturbed values. As it follows from Eq. (2) the mean volume reflection angle is a function of the bending radius and there is only one experiment which measured this function. Other experiments gave one or two measurements of characteristics. However, we include these results for the mean angle of volume reflection in our analysis, but we cannot do this for the mean square angle due to the absence of such data in measurements. However, the paper [12] demonstrates a good enough agreement in between for theoretical and measured values of the mean square angle.

Figure 2(a) and Table I show the results of measurements of the mean angle of volume reflection for the (110) silicon plane, which were obtained in different experiments and for different conditions such as the energy of the beam, the bending radius of the crystal and others. In the paper [2] it was predicted that the value $\Xi = \langle \alpha \rangle / \theta_c$ is a function of the variable R/R_0 where θ_c is the critical angle of channeling and $R_0 = \beta^2 E_0 d / U_0$ is some characteristic radius of the process. Some theoretical curves for Ξ are also presented here. The curves 1,2,3 are calculated in agreement with Eq. (2) for the (110) plane at the following conditions: the curve 1 is calculated for a thick enough silicon crystal when the integral in Eq. (2) is practically equal to its asymptotic value. The curve 2 is calculated for a tungsten thick crystal. One can expect that all crystals placed in the periodical table between silicon and tungsten are located between curves 1 and 2. The curve 3 is a calculation for 2 mm of length of the silicon crystal which was taken from Ref. [12]. The curve 4 is a simple approximation of the equation for volume reflection which was studied in Ref. [4]. This approximation as a function of the R/R_0-variable may be represented as

$$\frac{\langle \alpha \rangle (R/R_0)}{\theta_c} = \frac{\pi}{2} \left(1 - 2 \frac{R_c}{R_0} \frac{R_0}{R} \right) \quad (9)$$

where $R_c = E_0 / \mathcal{E}_{\max}$ is the critical radius and $\mathcal{E}_{\max}$ is the maximal value of the electric planar field [60.0 eV per angstrom for a (110) silicon plane]. We see that the curve 3 is in a good agreement with the experimental data. The curve 1 practically coincides with the curve 2 at small values (≤ 2) of the parameter R/R_0. The approximated curve 4 practically coincides with the curve 1. In the whole the curves 1 and 4 give a worse description of experimental data than the curve 3. Nevertheless, the curves 1 and 4 demonstrate a satisfactory enough agreement with measurements. Equation (9) (which corresponds to curve 4) is interesting due to its simplicity. This equation was obtained under the assumption that $R \gg R_c$ (see [4]) and it shows that for thick enough crystals (and at $R \gg R_c$) the ratio α/θ_c is a simple function of R/R_0.

As it follows from Table I the measurement and the calculation at 13 GeV differ by a sizeable quantity of about 10 μrad, for an estimate of the error of the experiment approximately equal to ± 4.7 μrad [17]. Besides, in this case the parameter $r_0 \approx 24$ and as it follows from Ref. [17] the scattered beam is the sum of two parts: the volume

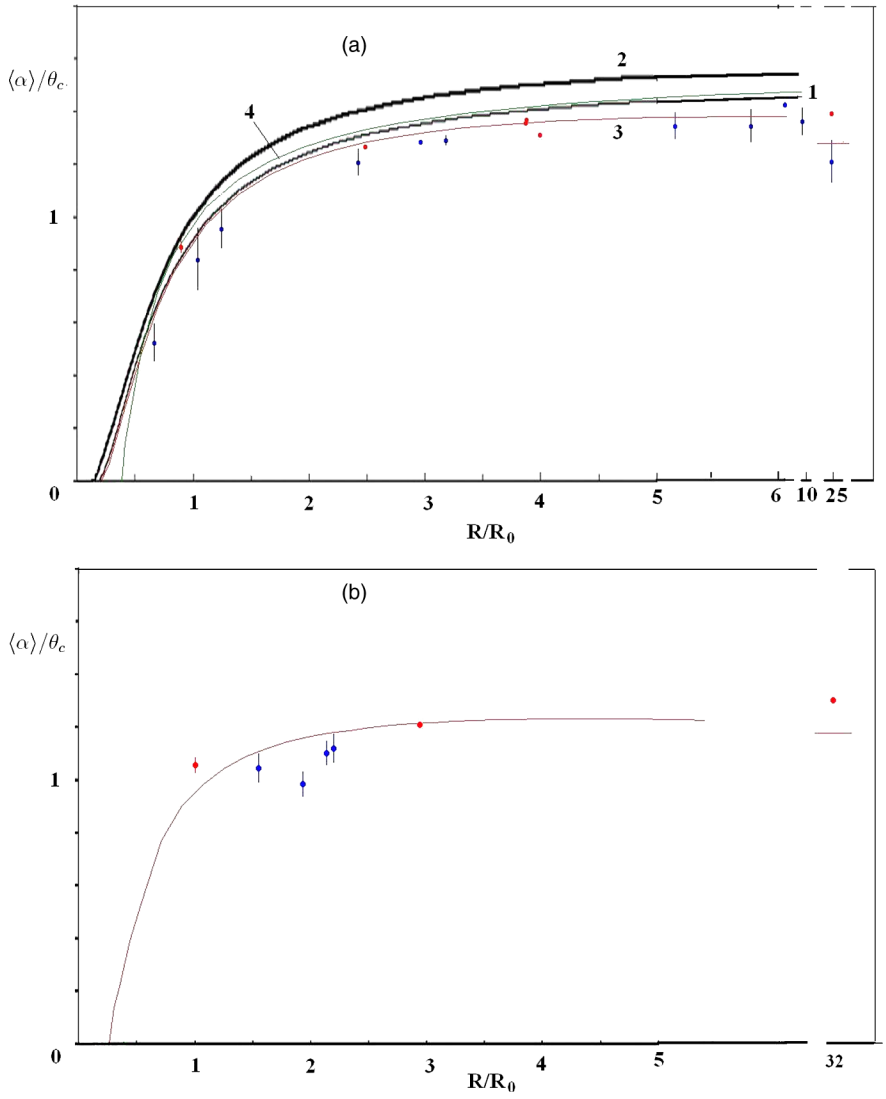

FIG. 2. Comparison between experimental and calculated mean angles of the volume reflection in the (110) (a) and (111) (b) planes of the bent silicon crystal. The red points correspond to recent measurements in Ref. [16]. For additional information, see the text.

reflected particles and volume captured one. Thus, the influence of volume capture may be strong enough and distort the comparison.

It should be noted that all our calculations for silicon were made with the use of the atomic potential obtained from x-ray experiments [20,21]. The mean volume reflection angle calculated by Eq. (2) with the assumption of the Moliere potential yield for it a larger absolute value, in comparison with results presented here. So, for example, the calculations based on Moliere model for silicon and for 400 GeV protons exceed by ≈ 0.75 μrad the analogous calculations with the help of the potential from X-ray measurements. This difference may be fixed experimentally. For elements with atomic numbers larger than the silicon atomic number the usage of Moliere potential is reasonable. It should be noted that several experimental points in Fig. 2 have very small error bars. This is due to the fact that we cannot find the systematic errors for these points.

In Table II and in Fig. 2(b) the results of calculations and measurements for volume reflection angle in the (111) silicon plane are presented. It is easy to see that there is a good enough agreement in these results. In our opinion the large difference for the angle at $R = 10.72$ m is connected with reasons such as the lack of perfection in the crystal and the like.

It should be noted that we present in Tables I and II and in Fig. 2 the new results which were recently obtained in the special experiment [16]. Most of these data show a very good agreement with theoretical calculations.

Recently, the experimental study of coherent processes in germanium single crystal were performed [23,24]. In Table III we carried out the comparison of experimental and calculated values of the planar mean angle of volume reflection for two strong planes in germanium at beam energy equal to 400 GeV. We have performed calculations for two different atomic potentials. The first one is the

TABLE I. Experimental data for mean volume reflection angle for (110) plane in bent silicon crystals. Here $\langle\alpha\rangle_c$ and $\langle\alpha\rangle$ are the calculated and measured values of the volume reflection angle.

E_0, GeV	l_0, mm	R, m	$\langle\alpha\rangle_c, \mu$rad	$\langle\alpha\rangle, \mu$rad	r_0	Ξ	Ref.
400	2	2.41	6.63	5.43	0.671	0.525	[12]
400	2	3.75	9.64	8.68	1.044	0.840	[12]
400	2	4.47	10.68	9.89	1.244	0.957	[12]
400	2	8.64	13.20	12.48	2.422	1.207	[12]
400	2	20.85	14.29	13.90	5.804	1.344	[12]
400	2	35.96	14.03	14.08	10.107	1.362	[12]
400	1.94	10.65	13.65	13.13	2.965	1.286	[17]
400	3	18.52	14.54	13.91	5.156	1.345	[15]
400	4	11.43	14.03	13.35	3.182	1.291	[18]
120	1.94	10.72	26.99	26.9	6.10	1.425	[17]
13	0.77	2.81	78.57	69.4	24.07	1.21	[19]
400	1.89	8.95	13.30	13.10	2.491	1.267	[16]
400	2.0	13.91	14.05	14.03	3.872	1.357	[16]
400	2.0	13.93	14.06	14.15	3.877	1.369	[16]
400	0.8	3.24	8.70	9.14	0.903	0.884	[16]
400	2.0	14.33	14.09	13.57	3.989	1.313	[16]
400	3.0	87.2	13.33	14.41	24.3	1.394	[16]

TABLE II. Experimental data for the mean volume reflection angle for (111) plane in bent silicon crystals. Here $\langle\alpha\rangle_c$ and $\langle\alpha\rangle$ are the calculated and measured values of the volume reflection angle at $E_0 = 400$ GeV.

E_0, GeV	l_0, mm	R, m	$\langle\alpha\rangle_c, \mu$rad	$\langle\alpha\rangle, \mu$rad	r_0	Ξ	Ref.
400	1.85	8.66	11.74	11.1	1.557	1.045	[15]
400	3	10.78	12.42	10.45	1.939	0.984	[15]
400	0.93	11.91	11.99	11.7	2.142	1.102	[22]
400	0.84	12.25	11.99	11.9	2.203	1.12	[22]
400	1.77	16.37	12.81	12.85	2.944	1.210	[16]
400	6.0	176.7	12.44	13.82	31.78	1.301	[16]
400	0.96	5.62	10.02	11.21	1.01	1.056	[16]

TABLE III. Experimental data for the mean volume reflection angle in bent germanium crystals. Here $\langle\alpha^*\rangle_c$, $\langle\alpha\rangle_c$ and $\langle\alpha\rangle$ are the calculated (for Moliere and Hartree-Fock approximations, correspondingly) and measured values of the volume reflection angle at $E_0 = 400$ GeV.$r_0 = R/R_0$ and $\Xi = \langle\alpha\rangle/\theta_c$, where θ_c corresponds to Hartree-Fock calculations.

Plane	R, m	$\langle\alpha^*\rangle_c, \mu$rad	$\langle\alpha\rangle_c, \mu$rad	$\langle\alpha\rangle, \mu$rad	r_0	Ξ	Ref.
(111)	15.0	18.50	17.2	15.9	6.33	1.224	[23]
(110)	2.3	14.78	12.85	11.4	1.00	0.864	[24]
(110)	8.2	20.05	18.67	17.3	3.57	1.311	[24]

Moliere potential [20,21] and the second one is taken from quantum mechanical calculations of the electron density based on the Hartree-Fock method [25].

For calculations we take the Debye temperature for the germanium crystal equal to ≈360 °K [26]. This temperature corresponds to mean square thermal atomic vibrations equal to 0.068 angstrom. From Table III we see a relatively good agreement between experimental values of the mean volume reflection angle and those calculated on the base of the Hartree-Fock approximation. In the case of the Moliere potential the difference between predicted and measured quantities is sizeable enough. The details of calculations of the volume reflection process for germanium will be presented elsewhere. For the Moliere potential we have $U_0 = 41.02, 41.96$ eV and for the Hartree-Fock approximation $U_0 = 34.82, 33.75$ eV for (110) and (111) planes, correspondingly.

TABLE IV. Experimental data for the mean volume reflection angle for negatively charged particles in bent silicon crystals. Here $\langle\alpha\rangle_c$ and $\langle\alpha\rangle$ are the calculated and measured values of the volume reflection angle at $E_0 = 400$ GeV.$r_0 = R/R_0$ and $\Xi = \langle\alpha\rangle/\theta_c$.

Plane	E_0, GeV	R, m	l_0, mm	$\langle\alpha\rangle_c, \mu$rad	$\langle\alpha\rangle, \mu$rad	r_0	Ξ	Ref.
(111)	150	12.92	0.84	14.28	14.64	10.12	0.84	[13]
(110)	150	22.79	0.98	11.81	11.53	16.92	0.68	[13]
(110)	120	2.71	2.0	11.13	11.4	2.64	0.60	[28]

In Table IV the comparison of the measurements of the mean volume reflection angle for negative particles with calculations is presented. We see a good enough agreement. However it is desirable to obtain more experimental data for the comparison.

One can find the computer program for calculations at [27].

III. VOLUME CAPTURE

Below we will demonstrate that for not so large values of bending radii the probability of volume capture is determined mainly by the motion (or behavior) of the particle on a relatively short distance (of the order of the interplanar distance in the transverse direction). Due to multiple scattering on atoms (at some conditions) the moving particle can lose transverse energy and make a transition from overbarrier motion into underbarrier motion (volume capture). Before studying the process of volume capture we propose a universal enough method for consideration of stochastic processes of a particle moving in crystals on short distances.

A. One-trajectory approximation of a diffusion process

Obviously, Eq. (1) reflects the conservation of the transverse energy. The introduction of multiple scattering violates this condition. Let us suppose that moving in the bent crystal one separate particle is scattered on the angle $\Delta\theta$ (by multiple scattering process). Then substituting this angle in Eq. (1) we get

$$\Delta E = E_0\beta^2\theta_m\Delta\theta + \frac{1}{2}E_0(\Delta\theta)^2. \quad (10)$$

Here $\theta_m \approx \dot{x}/c$ is the angle of the particle due to the regular motion in accordance with Eq. (1). Averaging over different values of $\Delta\theta$ we obtain the following equations:

$$\Delta E = \frac{1}{2}E_0(\Delta\theta)^2, \quad (11)$$

$$(E' - E - \bar{E})^2 = E_0^2\beta^4\theta_m^2(\Delta\theta)^2 = 4[E - U(x) - \beta^2 E_0 x/R]\Delta E \quad (12)$$

where E' is the transverse energy after multiple scattering and $\bar{E}$ is the mean energy losses of the transverse energy.

After averaging over different angles for different particles we get the distribution function over the changing transverse energy (from the distribution function over the plane scattered angle):

$$F(E', l) = \frac{1}{\sqrt{2\pi}\sigma_E}\exp -[(E' - E - \bar{E})^2/(2\sigma_E^2)], \quad (13)$$

where $\bar{E}$ and σ_E are expressed through the mean square angle of multiple scattering $\bar{\theta^2}$ (depending on the current depth l):

$$\bar{E} = \frac{1}{2}E_0\bar{\theta^2}, \quad (14)$$

$$\sigma_E^2 = E_0^2\beta^4\theta_m^2\bar{\theta^2}. \quad (15)$$

Note that the function F satisfies the following equation:

$$\frac{\partial F}{\partial l} = -\frac{d\bar{E}}{dl}\frac{\partial F}{\partial E'} + \frac{1}{2}\frac{d\sigma_E^2}{dl}\frac{\partial^2 F}{\partial E'^2}. \quad (16)$$

Thus we got a simple distribution function for one trajectory. This function depends on two parameters only: $\bar{E}$ and σ_E. These parameters are independent of the current transverse energy E'. It is clear that the approximation obtained here is valid on a short distance, when parameters $\bar{E}$ and σ_E are small enough in comparison with the characteristic value δE.

A more traditional consideration of a similar problem is based on the diffusion equation with the diffusion coefficients depending on the transverse energy. This fact strongly complicates the possibility for finding a solution.

B. Volume capture probability

Figure 1 illustrates the behavior of the effective potential $U_e(x) = U(x) + \beta^2 E_0 x/R$ as a function of the transverse coordinate x. The main problem of our consideration is the determination of an inefficiency of volume reflection of charged particles in bent single crystals. The mechanism of the inefficiency is connected with the volume capture process in these structures. Really, the moving particle has some probability to lose (because of multiple scattering) its transverse energy and to continue its motion in the channeling regime. However, the captured particle has some probability (due to dechanneling) to quickly return to overbarrier motion and to be similar to the usual particle at volume reflection. This fact requires the detailed description of the behavior of volume captured particles.

In this section we find the probability of volume capture. Figure 1 illustrates this process. Obviously the volume capture takes place mainly in the vicinity of the critical point. In Fig. 1 this region corresponds to $x_1 \le x \le x_c$ for transverse energies of the particle $E_m \le E \le E_M$. In Ref. [2] it was shown that particles of the beam with a small angle divergence in absence of multiple scattering are equiprobably distributed over transverse energies. Multiple scattering changes the initial particle distribution over transverse energies. However, the particle distribution in every energy period δE keeps approximately equiprobable. The evidence is similar to the case considered in Ref. [2].

We consider multiple scattering as in an amorphous medium, but instead of a constant nuclear density we use a variable one, in accordance with a current particle position. For this one can give different theoretical likelihood explanations, but a more evident argument is the fact that Monte Carlo calculations with the above mentioned assumptions give a good agreement with experiments.

Taking into account stated assumptions we define the probability of volume capture as an normalized number of particles (with the initial energy range from E_m till $E_M = E_m + \delta E$) which obtain (due to multiple scattering) the transverse energy corresponding to the finite planar motion (channeling).

As illustrated in Fig. 1 for every particle with the transverse energy $E_m \le E \le E_M$ and coming to coordinate x_1 there are three different possibilities (see numbers near curves in Fig. 1): (i) to undergo reflection; (ii) to lose the transverse energy and to become a particle captured in the channeling regime; (iii) to increase the transverse energy, so that $E > E_M$. In the case of number (iii) theoretically the similar three possibilities are conserved but for small enough bending radii the third variant is practically impossible. At the condition of smallness of the bending radius the probability for a particle (with $E_m \le E \le E_M$) to lose significantly the transverse energy before the coordinate x_1 is very small. Thus, we see that the volume capture probability can be represented as a sum of the two terms $\varepsilon_1 = \varepsilon_{1a} + \varepsilon_{1b}$, where ε_{1a} is the probability of volume capture in the coordinate range from x_1 till x_2 and ε_{1b} is the probability in the coordinate range from x_2 till x_3.

Let us calculate the first term ε_{1a}. Our consideration will be based on the one-trajectory approximation. Equation (5)

gives the distribution for one trajectory of the particle with the transverse energy E. The summary distribution function is a result of the integration over the whole range of transverse energies (from E_m till E_M). Taking this into account we get the probability to change the transverse energy E of a particle below the critical energy E_c in the following form:

$$\varepsilon_{1a} = \frac{1}{2} - \frac{1}{2}\int_0^1 \mathrm{erf}\left(\frac{\xi + \xi_m}{\sqrt{2}\Sigma}\right) d\xi, \tag{17}$$

where $\xi_m(\xi) = \bar{E}/\delta E$ and $\Sigma(\xi) = \sigma_E/\delta E$, $\bar{E}, \sigma_E$ are the mean and square mean losses of transverse energy [see Eqs. (14) and (15)], $\xi = (E - E_m)/\delta E$, $\delta E = E_0\beta^2 d/R$, $\mathrm{erf}(x) = 2/\sqrt{\pi}\int_0^x \exp(-t^2)dt$. One can write the following equations for the mean and mean square energy losses:

$$\bar{E} = 2A^2(L_0/X_0)/E_0^2, \tag{18}$$

$$\sigma_E = A\sqrt{2(L_1/X_0)}/E_0. \tag{19}$$

Here $A \approx 10$–14 MeV is the constant value, X_0 is the radiation length of a single crystal and L_0 and L_1 functions are

$$L_0 = \frac{E_0 c}{2\rho_0}\int_{t_1}^{t_2} \{\rho_a[x(t)] + \rho_e[x(t)]/Z^2\} dt, \tag{20}$$

$$L_1 = \frac{2E_0 c}{\rho_0}\int_{t_1}^{t_2} \{\rho_a[x(t)] + \rho_e[x(t)]/Z^2\} \times \{E - U[x(t)] - E_0\beta^2 x(t)/R\} dt, \tag{21}$$

where $\rho_a(x), \rho_e(x)$ are the planar atomic and electron densities for a selected plane of single crystal, Z is the atomic number, $\rho_0 \approx N_0/V_0$ is the mean atomic density (N_0 is number atoms in a fundamental cell of volume V_0). Here t_1 is the time which corresponds to finding of particle in the nearest local maximum of U(x) before critical point x_c (for this particle). The time t_2 corresponds to the location of the particle in a critical point. The coefficient 2 in Eqs. (18) and (19) is due to the symmetry of the particle motion before and after a critical point.

Taking into account the relation:

$$dt = \frac{dx}{\sqrt{\frac{2c^2}{E_0\beta^2}[E - U(x) - E_0\beta^2 x/R]}}, \tag{22}$$

we can represent Eqs. (11) and (12) in the following form:

$$\bar{E} = \frac{A^2}{\sqrt{2E_0}\rho_0 X_0}\int_{x_1}^{x_c} \frac{[\rho_a(x) + \rho_e(x)/Z^2]}{\sqrt{E - U(x) - E_0\beta^2 x/R}} dx, \tag{23}$$

$$\sigma_E = \frac{2^{\frac{3}{4}}A}{E_0^{\frac{1}{4}}(\rho_0 X_0)^{\frac{1}{2}}}\left\{\int_{x_1}^{x_c} [\rho_a(x) + \rho_e(x)/Z^2] \times \sqrt{E - U(x) - E_0\beta^2 x/R} dx\right\}^{\frac{1}{2}}. \tag{24}$$

It is convenient to rewrite Eqs. (23) and (24) in the following more general form:

$$\bar{E} = \frac{A^2 d}{\sqrt{2E_0 U_0}\rho_0 X_0}\int_{y_1}^{y_c} \frac{[\rho_a(y) + \rho_e(y)/Z^2]}{\sqrt{\nu/\kappa - U(y)/U_0 - y/\kappa}} dy = \frac{A^2 d}{\sqrt{2E_0 U_0}X_0} f_1(\nu, \kappa), \tag{25}$$

$$\sigma_E = \frac{2^{\frac{3}{4}}AU_0^{\frac{1}{4}}d^{\frac{1}{2}}}{E_0^{\frac{1}{4}}(\rho_0 X_0)^{\frac{1}{2}}}\left\{\int_{y_1}^{y_c} [\rho_a(y) + \rho_e(y)/Z^2] \times \sqrt{\nu/\kappa - U(y)/U_0 - y/\kappa} dy\right\}^{\frac{1}{2}} = \frac{2^{\frac{3}{4}}AU_0^{\frac{1}{4}}d^{\frac{1}{2}}}{E_0^{\frac{1}{4}}X_0^{\frac{1}{2}}} f_2(\nu, \kappa), \tag{26}$$

where $y = x/d$, U_0 is the potential barrier of plane for a straight single crystal and the parameter $\kappa = U_0 R/(E_0\beta^2 d)$. This dimensionless parameter can be represented also as $\kappa = R/R_0$, where $R_0 = \beta^2 E_0 d/U_0$ is the characteristic radius of volume reflection [2]. Another dimensionless parameter is $\nu = E/\delta E$. The parameter ν is coupled with the ξ-parameter [see Eq. (17)] by the relation: $\xi = \nu - \nu_m = (E - E_m)/\delta E$, where E_m is the nearest local maximum of the transverse energy before the critical point x_c ($\nu_m = E_m/\delta E$). Note that the functions $\bar{E}(\xi)$ and $\sigma_E(\xi)$ are periodic functions of the ξ-variable with the period equal to 1.

The distribution of scattered particles over the relative transverse energy $\xi' = (E' - E_m)/\delta E$ follows from integration of Eq. (13):

$$\mathcal{F}_a(\xi') = \frac{dN(\xi')}{d\xi'} = \frac{1}{\sqrt{2\pi}}\int_0^1 \frac{d\xi}{\Sigma}\exp - \frac{(\xi' - \xi - \xi_m)^2}{2\Sigma^2}. \tag{27}$$

This function describes all scattered particles at $-\infty < \xi' < \infty$. The case $\xi' < 0$ corresponds to particles with $E' < E_m$ and the case $\xi' > 1$ corresponds to particles with $E' > E_M$. It is significant to note that here and below (in similar equations) the values ξ_m and Σ are functions of the integration variable. Integration of Eq. (27) at the condition $\xi' < 0$ gives Eq. (17) for the total number particles, and at the condition $\xi' > 1$ it gives the corresponding total number of particles with $E > E_M$:

$$\varepsilon_0 = \frac{1}{2} - \frac{1}{2}\int_0^1 \mathrm{erf}\left(\frac{1-\xi-\xi_m}{\sqrt{2}\Sigma}\right) d\xi. \tag{28}$$

The distribution of captured particles (due to the additional process, see the trajectory 3 in Fig. 1) reads

$$\mathcal{F}_b(\xi'') = \frac{1}{\sqrt{2\pi}}\int_1^\infty \mathcal{F}_a(\xi')\frac{\exp[-(\xi''-\xi'-\xi_m)^2/(2\Sigma^2)]}{\Sigma} d\xi'. \tag{29}$$

Here $\xi'' < 1$, $\xi' = (E' - E_m)/\delta E$, $\xi'' = (E'' - E_m)/\delta E$, where E' and E'' are the corresponding transverse energies (see Fig. 1). Thus, the total number of captured particles, normalized on unit, in this approximation is $\varepsilon_1 = \varepsilon_{1a} + \varepsilon_{1b}$, where $\varepsilon_{1b} = \int_{-\infty}^1 \mathcal{F}_b d\xi''$. Note that our consideration of volume capture is valid for small enough bending radii of single crystals. The range of applicability of the present description will be studied below.

C. Channeling of the captured particles

For some time the captured particles move in a planar channel, but due to multiple scattering (in the channeling regime) these particles obtain transverse energies which exceed the potential barrier, and hence a part of them return in overbarrier motion. In this section we consider this process on the basis of the one-trajectory diffusion approximation.

For calculations we need to know the losses of transverse energy of a channeled particle. For this aim we can use Eqs. (25) and (26). However, we should put the transverse energy $E_m - U_R < E < E_m$ at the location of particles in the range $x_1 < x < x_c$ ($U_R = E_m - E_{\mathrm{ch}}$, see Fig. 1). At this condition a particle will be in the channeling regime. At first, we find the mean and mean square losses of the transverse energy per one period of motion l_c (l_c is a function of a transverse energy). Then we can get approximately that these losses depend on the factor l/l_c [see Eqs. (18)–(21)], where l is the length of a single crystal. We think that, for $l/l_c > 1$, this approximation is good enough.

Now we find the distribution function of the channeling fraction:

$$\mathcal{F}_c(\xi'', l) = \frac{1}{\sqrt{2\pi}}\int_{\approx -U_R/\delta E}^0 [\mathcal{F}_a(\xi') + \mathcal{F}_b(\xi')]\frac{\exp[-(\xi''-\xi'-\xi_{mc})^2/(2\Sigma_c^2)]}{\Sigma_c} d\xi' \tag{30}$$

where $\xi_{mc} = (l/l_c)\bar{E}/\delta E$ and $\Sigma_c = \sqrt{l/l_c}\sigma_E/\delta E$ and the variables ξ' and ξ'' are similar to the analogous ones in Eq. (29). Note that, due to the periodicity of the process, we wrote ξ'-value as the argument of $\mathcal{F}_b$-function (instead of $\xi' + 1$). Obviously this equation is valid for small enough l-values while the captured particles have transverse energies larger than $E_m - U_R$.

Integration of $\mathcal{F}_c(\xi'')$-function over ξ'' (from $\approx -U_R/\delta E$ till 0) gives the normalized number of channeling particles $\varepsilon_2(l)$.

IV. ANGLE DISTRIBUTION OF SCATTERED PARTICLES

Relations describing the angle distributions of scattered particles in the process of volume reflection were obtained in Ref. [2]. However, these relations do not take into account the volume capture. If we want to take into account this factor we should divide all particles in two sorts. The first sort is the particles which were not captured and the second one is the captured particles. The number of particles of the first sort is $1 - \varepsilon_1$ and the number of particles of the second sort is ε_1. The summary angle distribution of particles may be represented as $dN_T(\alpha)/d\alpha = dN_{vr}(\alpha)/d\alpha + dN_{vc}(\alpha)/d\alpha$, where $dN_{vr}/d\alpha$ is the angle distribution of pure volume reflected particles (see the detailed description in Ref. [2]) and $dN_{vc}/d\alpha$ is the angle distribution of volume captured particles.

Let us consider a bent single crystal of the finite thickness l_0. Then the volume captured particles can be represented as a sum of two fractions: the first fraction N_{ch} is the particles which enter from a single crystal in the channeling regime (underbarrier motion) and the second one N_{de} is the particles which are transmitted from channeling in overbarrier motion (due to the dechanneling mechanism). Let us suppose that the normalized number particles of the first fraction is ε_2, then the normalized number of particles in the second fraction is equal to $\varepsilon_1 - \varepsilon_2$.

In Ref. [2] the term "physically narrow angle distribution of entering particles" was introduced. This term means that the characteristic size of the angle distribution of the entering particles exceeds the angle period $\delta\theta = d/(R\theta)$ (here θ is the initial angle of the particle) and particles are uniformly distributed within this period. Up to this point we considered the multiple scattering only in a narrow range of transverse coordinate [$< d$, see Eqs. (25) and (26)]. In this approximation we can write

$$\frac{dN_{\mathrm{de}}(\alpha)}{d\alpha} = \frac{d\varepsilon_2(\phi)}{d\varphi}\vartheta(\varphi_{\max} - \varphi)\vartheta(\varphi). \tag{31}$$

Here $\phi = -\alpha_m/2 + \varphi$ and α_m is the mean angle of volume reflection, and angle $\varphi = (l - l_0/2)/R$, where $\varphi_{\max} = l_0/(2R)$, and $\vartheta(x) = 1$ or 0 at $x > 0$ and $x < 0$), respectively. The function $\varepsilon_2(l)$ is determined after Eq. (30). The presented equation is valid for the symmetric case of orientation of a single crystal. Note that the case of nonsymmetric orientation is considered analogously.

Figure 1(b) illustrates the geometry for Eq. (31). Here the broken line COD represents the motion of a particle due to volume reflection. The lines CE and OD are the directions of the particle motion before and after the process. The angle DOE is the mean angle of volume reflection. AB is a tangent line in the critical point. We define the direction along the CE-line as the zero angle (the initial direction of the particle motion). It means that the angle between the OD- line (the direction of volume reflection) and the current direction of the channeling flux is approximately equal to $\alpha = -\alpha_m/2 + \varphi$ [see Eq. (31)].

For the final result we should take into account multiple scattering in the body of a single crystal. In accordance with Ref. [2] we get

$$\left\langle \frac{dN_{\rm de}}{d\alpha}(\alpha) \right\rangle = \int_{-\infty}^{\infty} \rho(\varphi, \sigma_{ms}) \frac{dN_{\rm de}}{d\alpha}(\alpha - \varphi) d\varphi \qquad (32)$$

where $\rho(\varphi, \sigma_{ms})$ is the distribution function of multiple scattering with σ_{ms} corresponding to the thickness $l_0/2 - (l - l_0/2)\vartheta(l - l_0/2)$, $l = \varphi R - l_0/2$ ($l - l_0/2$ is the part of particle path in the body of the single crystal which corresponds to the motion in the channeling regime).

In our model the process of volume capture takes place in the transverse space from x_1 up to x_3 (see Fig. 1). It corresponds to the δ-function distribution of the captured particles. In reality, multiple scattering distributed this process in some transverse area and hence in some longitudinal space. One can describe the evolution of the distribution of volume captured particles with the help of the function [2]:

$$\frac{dN_{\rm ca}}{dl} = \frac{\varepsilon_1}{\sqrt{2\pi}\sigma_{\rm ca} R} \exp - \frac{(l_0/2 - l)^2}{2\sigma_{\rm ca}^2 R^2} \qquad (33)$$

where $\sigma_{\rm ca}$ is the mean squared angle of multiple scattering corresponding to approximately half of the single crystal thickness.

The density of dechanneling particles as a function of the length l (or the angle φ) is described by a relation like Eqs. (31) and (32) (at the condition $\alpha_m = 0$) but for σ_{ms} should be taken for a length equal to $l_0/2$. It means that we consider particles in the vicinity of the local variable l and do not take into account further motion in the body of a single crystal. Let us denote this function as $dN_{\rm de0}/dl$ (or $dN_{\rm de0}/d\varphi = R dN_{\rm de0}/dl$).

Now we can describe the behavior of the channeling fraction as a function of the length (or the angle φ) by the following equation:

$$\varepsilon_2(l) = N_{\rm ch}(l) = \int_0^l \left[\frac{dN_{\rm ca}}{dl}(z) - \frac{dN_{\rm de0}}{dl}(z) \right] dz \qquad (34)$$

Next, we can find the angle distribution of the channeling fraction. It is easy to get the velocity $[v(t) = \dot{x}(t)]$ distribution function (normalized to 1) of channeled particles for a fixed transverse energy E:

$$\frac{dN}{dv}(v) = \frac{E_0}{\tau c^2 |\beta^2 E_0/R - \mathcal{E}[x(t)]|} \qquad (35)$$

where τ is one half of the period of the motion for the channeled particle and $\mathcal{E}$ is the intensity of the planar electric field. Taking into account that $\theta \approx v/c$, we can recalculate this distribution in angle. Knowing the distribution function over the transverse energy of channeled particles [see Eq. (30)] we can find the resulting distribution of these particles at the exit from a crystal.

V. EXAMPLES OF CALCULATIONS

A. Introduction remarks

In this section, in accordance with obtained equations, we present calculations of the volume reflection process, which take into account the processes of volume capture and channeling in bent single crystals. For illustration we selected some energies of proton beams which approximately correspond to energies of well-known accelerators. The main and detailed calculations were carried out for silicon single crystals, but some results were obtained for some different kind of single crystals. For the calculation of the potential, electric field, electron and atomic densities in silicon we use values of atomic form factors from x-ray experiments. The method of calculations can be found in Refs. [20,21]. Note that recent experimental data [18] show that the potential from x-ray diffraction gives a more precise description of measured characteristics of volume reflection for a silicon single crystal than the Moliere potential.

Formally, our consideration of volume capture may be also applied for negatively charged beams. However, due to the importance of possible applications of volume reflection, we concentrate our specific calculations only for positively charged particles.

B. Energy losses for over and underbarrier particles

For the determination of different distribution functions we should know the mean and mean squared energy losses of particles [see Eqs. (25) and (26)]. Figure 3 illustrates these quantities for over and underbarrier motion of 400 GeV/c protons. For these calculations we use $A = 11$ MeV [see Eqs. (18) and (19)]. This choice was based on the equation for the mean square angle of multiple scattering [29] $\theta_{\rm ms} = 13.6\,[\text{MeV}]/\beta c p \sqrt{l/X_0}[1 + 0.038 \ln(l/X_0)]$, where p is the particle momentum. For a small thickness l $l/X_0 \approx 10^{-3}$ and the more natural law $\theta_{\rm ms} = A/E_0\sqrt{l/X_0}$ the best agreement is at $A = 11$ MeV.

It is easy to recalculate the results of Fig. 3 for any energy of particles [see Eqs. (25) and (26)]. The numerical values of universal functions f_1 and f_2 can be also found from Fig. 3.

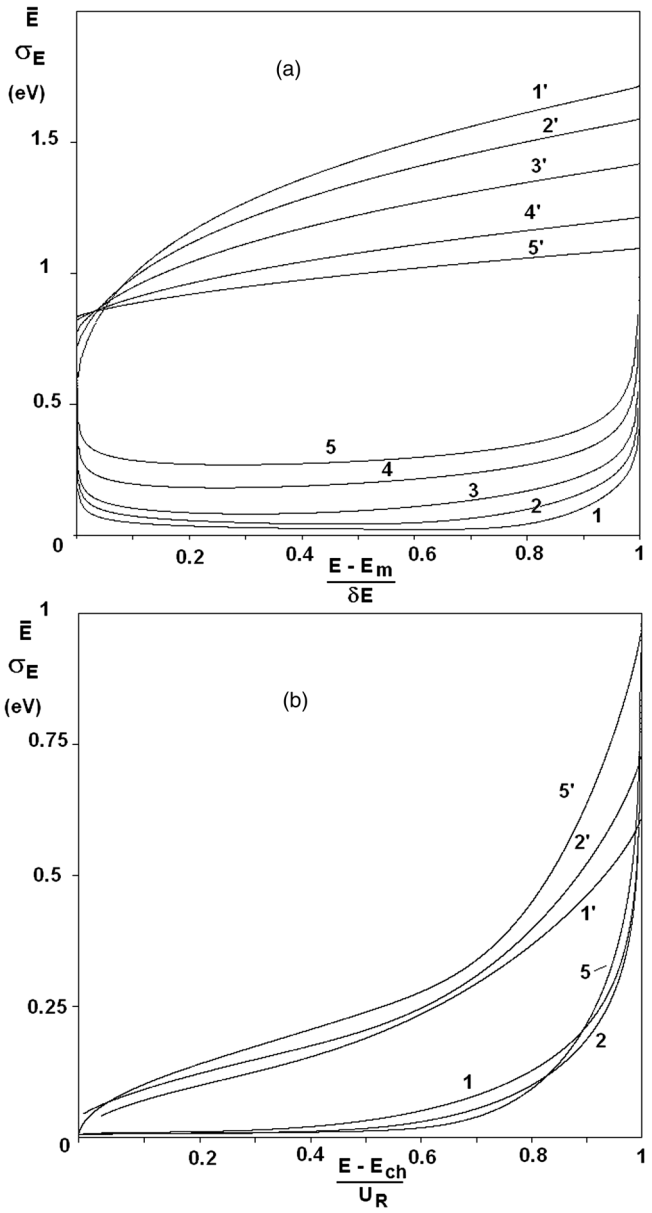

FIG. 3. Losses of transverse energies $\bar{E}$ and σ_E [in the (110) silicon plane] for volume reflection (a) and for channeling regime (b) as functions of variables $(E - E_m)/\delta E$ and $(E - E_{\mathrm{ch}})/U_R$, correspondingly. The numbers 1–5 near curves are equal to the value of the κ-parameter and correspond to $\bar{E}$-quantities. Analogously the numbers $1'$–$5'$ are equal to the value of the κ-parameter and correspond to σ_E-quantities. The values $\bar{E}$ in (b) are enlarged by three times for good visibility. The particle energy is equal to 400 GeV.

C. Simulations of volume capture

The volume capture probability represents the sum of two terms $\varepsilon_1 = \varepsilon_{1a} + \varepsilon_{1b}$. Initially we consider the behavior of the first term ε_{1a}. Figure 4 illustrates the calculations of this value for different proton energies. One can see that at small values R/R_c ε_1 is approximated well enough by a linear function. It is useful to find the form of this linear function.

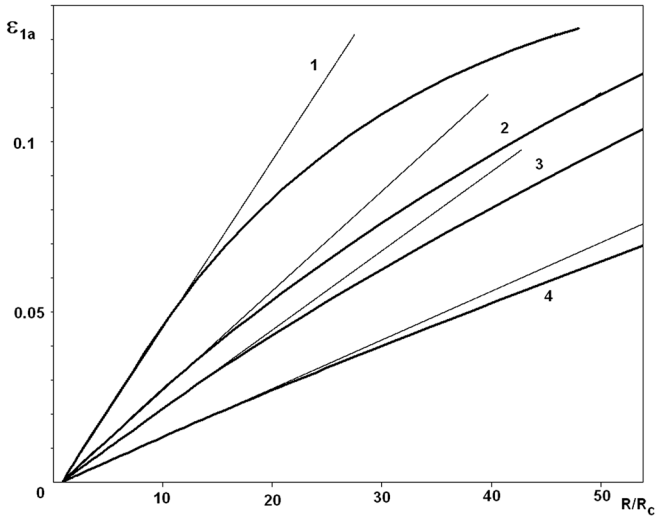

FIG. 4. The partial probability of volume capture ε_{1a} [see Eq. (17) for the (110) silicon plane as a function of the relation R/R_c for different energies 50 GeV (1), 400 GeV (2), 1000 GeV (3), 7000 GeV (4). The straight lines near curves are linear approximations (see Eq. (36)].

The probability ε_{1a} can be presented as the sum of the two first terms of the Taylor series in the vicinity of κ_{oo}:

$$\varepsilon_{1a}(\kappa) = \varepsilon_{1a}(\kappa_{oo}) + \frac{d\varepsilon_{1a}}{d\kappa}(\kappa_{oo})\kappa_c\left(\frac{\kappa}{\kappa_c} - \frac{\kappa_{oo}}{\kappa_c}\right), \qquad (36)$$

where $\kappa_c = U_0 R_c/(E_0\beta^2 d)$ and $R_c = E_0/\mathcal{E}_{\max}$ is the critical radius of channeling ($\mathcal{E}_{\max}$ is the maximal value of the interplanar electrical field). Thus, $\kappa_c = U_0/(\mathcal{E}_{\max} d)$ and $\kappa/\kappa_c - \kappa_{oo}/\kappa_c = R/R_c - R_{oo}/R_c$ (radius $R_{oo} \geq R_c$ corresponds to κ_0-value). The presentation of a bending radius in units of critical radius is convenient for the consideration of the process at different particle energies.

From Eq. (17) one can get

$$\frac{d\varepsilon_{1a}}{d\kappa} = -\frac{1}{\sqrt{2\pi}}\int_0^1 \frac{\xi_m}{\Sigma}\left[\frac{f_1'}{f_1} - \frac{f_2'}{f_2} - \frac{\xi}{\xi_m}\left(\frac{1}{\kappa} + \frac{f_2'}{f_2}\right)\right] \times \exp[-(\xi + \xi_m)^2/(2\Sigma^2)]d\xi, \qquad (37)$$

where f_1', f_2' are the corresponding derivatives (of the f_1, f_2 -functions) over the κ-parameter.

Taking into account Eqs. (25) and (26) one can represent Eq. (37) in the following form:

$$\frac{d\varepsilon_{1a}}{d\kappa}(\kappa_{oo})\kappa_c = \frac{A U_0^{\frac{1}{4}}}{2^{\frac{7}{4}}\sqrt{\pi}E_0^{\frac{1}{4}}\mathcal{E}_{\max} d^{\frac{1}{2}} X_0^{\frac{1}{2}}} J(\kappa_{oo}), \qquad (38)$$

where

$$J(\kappa_{oo}) = -\int_0^1 \frac{f_1}{f_2}\left[\frac{f_1'}{f_1} - \frac{f_2'}{f_2} - \frac{\xi}{\xi_m}\left(\frac{1}{\kappa_{oo}} + \frac{f_2'}{f_2}\right)\right] \times \exp[-(\xi + \xi_m)^2/(2\Sigma^2)]d\xi. \qquad (39)$$

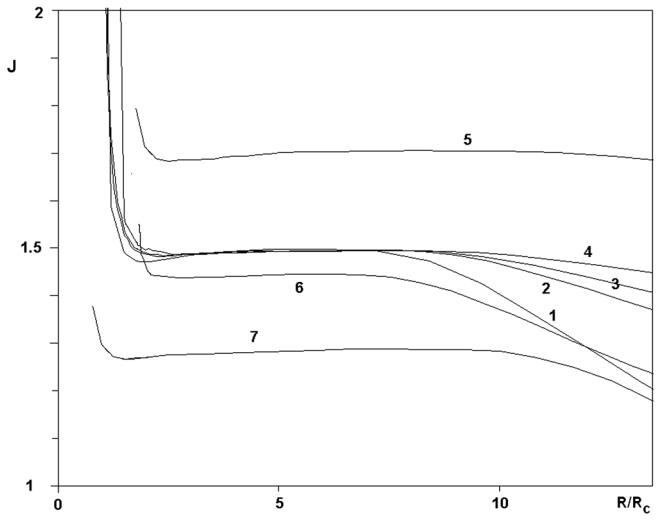

FIG. 5. J-value [see Eq. (38)] as a function of the relation R/R_c for different conditions. Curves 1,2,3,4 are for a silicon single crystal and proton energies 50, 400, 1000, and 7000 GeV, respectively. Curves 5,6,7 are for diamond, germanium, and tungsten single crystals and proton energy equal to 400 GeV.

From Eq. (38) we see that the value $\kappa_c d\varepsilon_{1a}/d\kappa$ is defined by the $J(\kappa_{oo})$-integral. Figure 5 illustrates the calculated J-value as a function of $\kappa_{oo} = R_{oo}/R_c$. We see a long enough plateau beginning from κ_{oo} slightly larger than κ_c. It is convenient to select a κ_{oo} such that $\varepsilon_{1a}(\kappa_1) = 0$, where we denote this special value of κ_{oo}- set as κ_1. It is easy to see that

$$\kappa_1 = \kappa_{oo} + \frac{\varepsilon_{1a}(\kappa_{oo})}{\frac{d\varepsilon_{1a}}{d\kappa}(\kappa_{oo})}, \tag{40}$$

where κ_0 is any value of κ in the range of linearity of the ε_{1a} function. According to our calculation for the silicon (110) plane $\kappa_1 \approx 0.13$. Now we can write the following relation:

$$\bar{\varepsilon}_{1a} = \frac{AU_0^{\frac{1}{4}} J_p}{2^{\frac{7}{4}}\sqrt{\pi} E_0^{\frac{1}{4}} \mathcal{E}_{\max} d^{\frac{1}{2}} X_0^{\frac{1}{2}}} \left(\frac{\kappa}{\kappa_c} - \frac{\kappa_1}{\kappa_c}\right) \tag{41}$$

Here we denote the linear approximation of ε_{1a} [see Eq. (17)] as $\bar{\varepsilon}_{1a}$ and the plateau value of J as J_p.

We calculated also the value ε_{1b} [see Eq. (29)] for different crystals. According to these calculations the relation $\varepsilon_{1b}/\varepsilon_{1a}$ is approximately equal to 0.41- 0.37 at $R/R_c = 1.5$–30, correspondingly. We think that we can decide this relation to be approximately constant in this region of radii and equal to 0.39. Then we can write the final equation for the probability ε_1:

$$\bar{\varepsilon}_1 \approx \frac{1.39AU_0^{\frac{1}{4}} J_p}{2^{\frac{7}{4}}\sqrt{\pi} E_0^{\frac{1}{4}} \mathcal{E}_{\max} d^{\frac{1}{2}} X_0^{\frac{1}{2}}} \left(\frac{\kappa}{\kappa_c} - \frac{\kappa_1}{\kappa_c}\right) \tag{42}$$

Analogously, here $\bar{\varepsilon}_1$ denotes the linear approximation of ε_1.

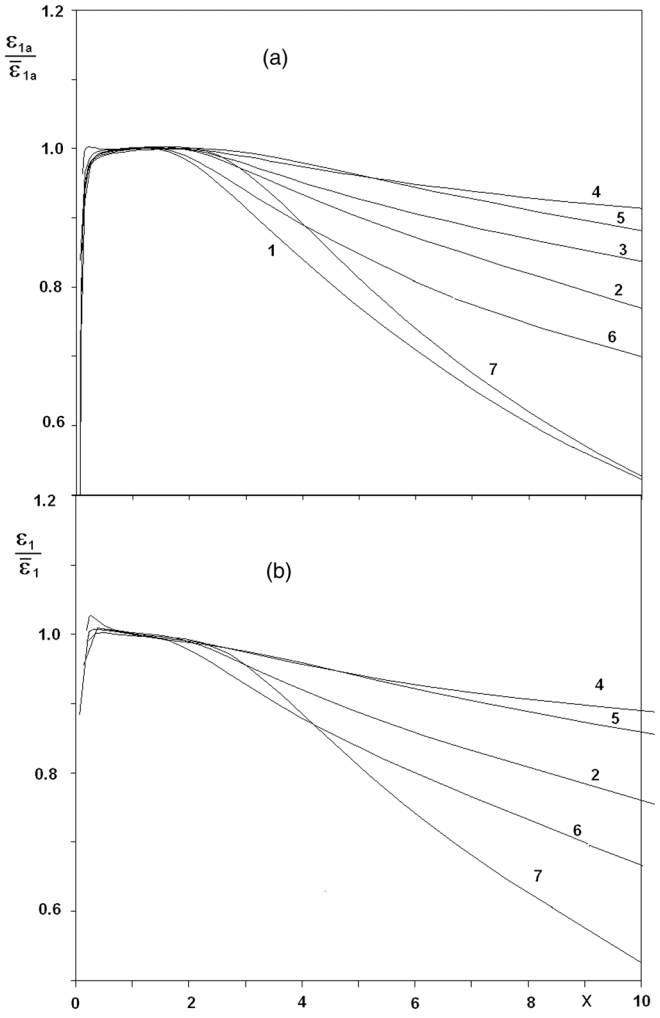

FIG. 6. The relations $\varepsilon_{1a}/\bar{\varepsilon_{1a}}$ (the partial probability of volume capture to its linear approximation) (a) and $\varepsilon_1/\bar{\varepsilon_1}$ (the total probability of volume capture to its linear approximation) (b) as functions of the x-value, where $X = (R/R_c - \kappa_1)/\kappa_c$ and κ_1, κ_c-values are taken from Table V (see text). Numbers near curves are the same as in Fig. 5.

Figure 6 illustrates the behavior of the relations $\varepsilon_1/\bar{\varepsilon}_1$ and $\varepsilon_{1a}/\bar{\varepsilon}_{1a}$ as functions of the variable $X = (\kappa - \kappa_1)/\kappa_c$. One can see that in the region from $X = 0.2$ till ≈ 2.5 these relations are constant with a good enough accuracy. Thus, Eq. (42) allows one to describe in a universal way the probability of volume capture in the area of interest to us. Table I contains the parameters of some single crystals for the calculation of the ε_1-value.

Figure 7 illustrates the differential over energy distributions of captured protons calculated with the help of Eqs. (27) and (29). We see that these distributions become more wide with the increasing of the bending radius.

D. Channeling of captured particles

We illustrate the channeling of captured particles for proton energy 400 GeV and 10 m bending radius for the

TABLE V. Parameters of single crystals for the calculation of the volume capture probability [see Eq. (42)]. Potentials for diamond and silicon are taken from x-ray measurements [20,21] and for germanium and tungsten the Moliere potential was used.

Crystal	Z	X_0, cm	d, A	U_0, eV	$\mathcal{E}_{\max}$, eV/A	κ_c	κ_1	J_p
C(diamond)	6	12.14	1.26	23.52	79.70	0.234	0.198	1.71
Si	14	9.38	1.92	21.38	60.0	0.186	0.13	1.49
Ge	32	2.28	2.00	41.02	111.46	0.183	0.123	1.44
W	74	0.383	2.23	138.34	490.3	0.126	0.0085	1.29

(110) plane of a silicon single crystal. Similar simulations based on Monte Carlo calculations for these parameters were presented in Ref. [6]. Hence, we can compare results which were carried out by different methods. Equation (34) allows one to calculate the flux of particles which were captured in the channeling regime. Figure 8 shows the behavior of the flux as a function of the thickness of a crystal. The curves 1 and 2 [see Fig. 8(b)] present the speed of dechanneling as a function of the variable bending angle for cases without and with consideration of multiple scattering in a silicon crystal (more exactly, for curve 1 multiple scattering takes place in a narrow region of coordinate x [$x_1 \le x \le x_2$, see Fig. 1)] In this figure the curve 3 presents the distribution function of dechanneling particles at the exit of a single crystal. The total number of captured particles is ≈0.057. The same number is ≈0.064 according to Ref. [6].

E. Total scattering curve

Thus, the total scattering curve (with taking account of the volume capture process) represents the sum of three curves:

(i) the pure volume reflection curve;
(ii) the curve of the dechanneling fraction;
(iii) the curve of the channeling fraction.

The resulting curve [for 400 GeV protons and 10 m bending radius of (110) plane silicon single crystal] is shown in Figs. 9 and 10 in linear and logarithmic scales, correspondingly. The curve of the channeling fraction was calculated in accordance with Eq. (39). The semi-period in Eq. (39) was chosen under the condition that at the moment of time t_1 the transverse velocity is maximal

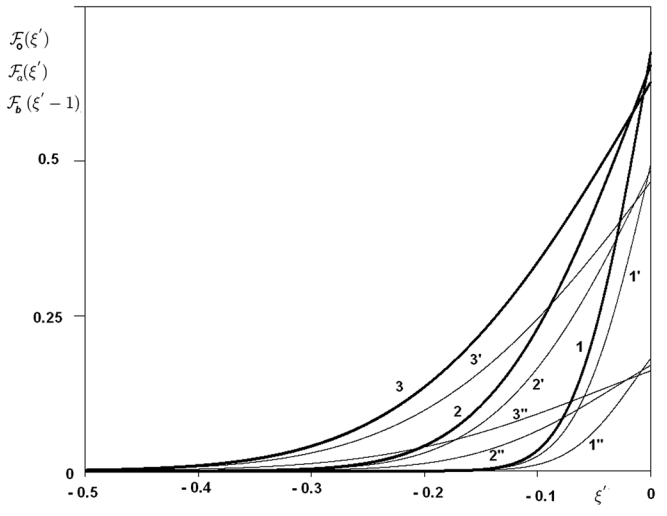

FIG. 7. The total and partial distributions $\mathcal{F}_0, \mathcal{F}_a, \mathcal{F}_b$ as functions of the ξ-parameter for bending radii equal to 5, 10, 15 m (curves 1,2,3, respectively). Here ξ-parameter represents mean energy losses $\bar{E}$ of particle at volume reflection in units of the transverse energy period δE. $\mathcal{F}_0 = \mathcal{F}_a + \mathcal{F}_b$. The curves labeled as $'$ and $''$ correspond to $\mathcal{F}_a, \mathcal{F}_b$ -distributions and the thick curves to the $\mathcal{F}_0$ one. The energy of a proton beam is equal to 400 GeV.

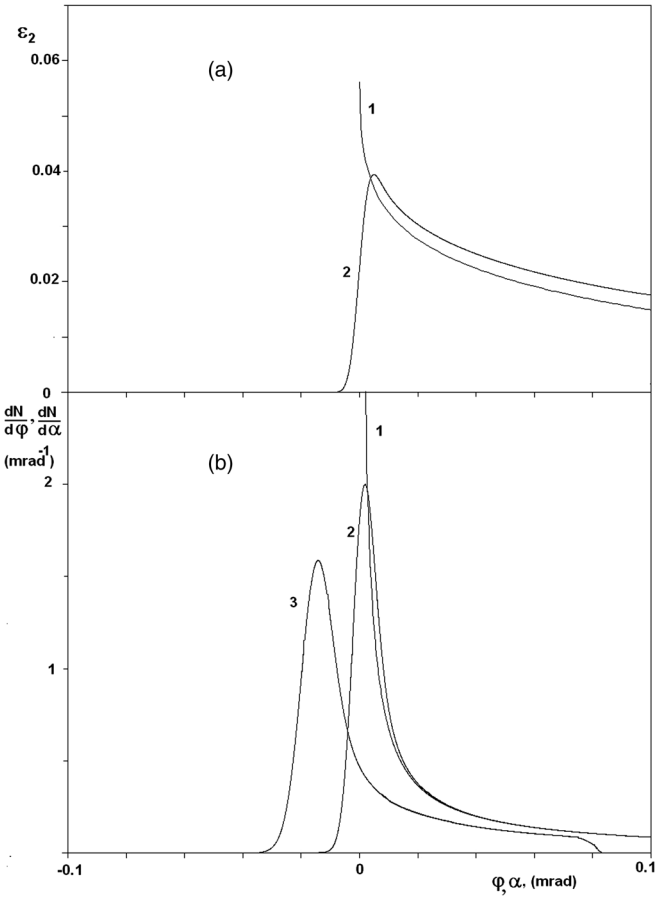

FIG. 8. Intensity of channeling fraction (a) and differential particles losses due to dechanneling (b) as functions of the angle φ. Curves 1 and 2 correspond to considerations without and with multiple scattering. Curve 3 corresponds to the angle distribution (over α-angle) dechanneling fraction on the entrance of a single crystal.

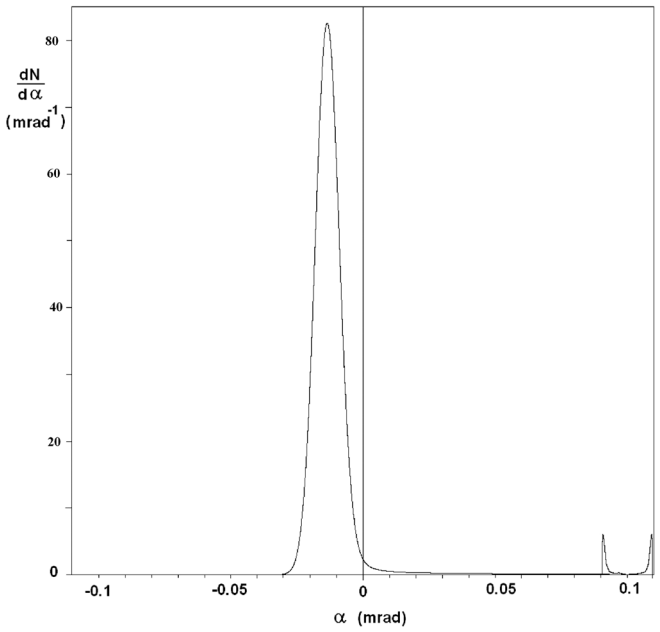

FIG. 9. The resulting distribution of scattered particles at volume reflection taking into account the influence of volume capture. The energy of protons is equal to 400 GeV, the bending radius of a 2-mm silicon single crystal is equal to 10 m.

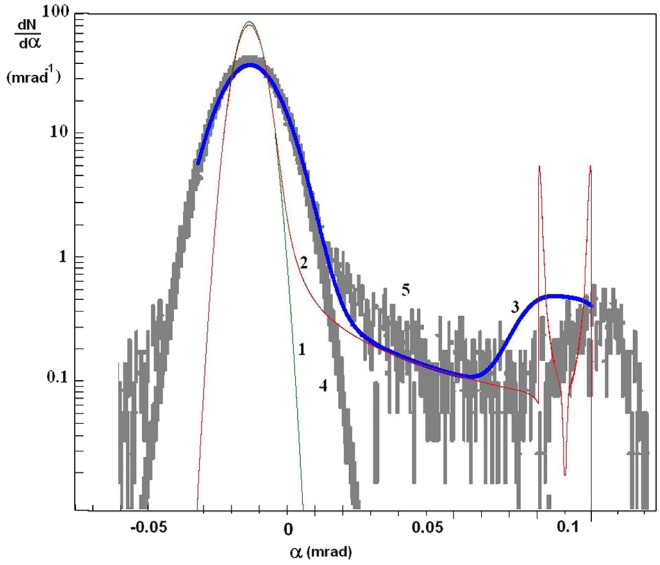

FIG. 10. The distributions (in logarithmic y-scale) of scattered particle at volume reflection of 400 GeV protons in (110) planes of silicon single crystal. The curve 1 is calculated for parallel beam without consideration of diffusion process (the transverse energy is conserved); the curve 2 is a calculation in which the influence of volume capture on a process taken into account; the curve 3 is a calculation in which the influence of volume capture and divergence of proton beam on a process taken into account; the curve 4 is the Gaussian approximation of experimental scattering curve; the curve 5 is the full experimental scattering curve. For additional information, see the text.

and at the moment of time $t_2 = t_1 + \tau$ this velocity is minimal.

One can see that, in accordance with the distribution function, most particles of the channeling fraction are grouped near the critical channeling angle. This fact is due to the fact that first, a large number of particles have a high transverse energy and second, the time of stay in a state with small transverse velocity is considerably larger than the time of stay in a state with a large velocity. It should be noted that the experimental observation of two peaks of the channeling curve is practically impossible because of multiple scattering in detectors.

The important characteristics of volume reflection of a beam is the efficiency of the process which is defined as a partition of the beam which is contained in $\pm 3\sigma_{vr}$ around the mean angle of reflection α_m, where σ_{vr} is the mean square of the angle distribution of the scattered beam. For the conditions calculated as in Figs. 9 and 10 the efficiency is close to 0.98. This is in agreement with the experimental data [15]. From this result it follows that, for the above mentioned definition of the efficiency ε, the total inefficiency $(1-\varepsilon)$ should be significantly less than the probability of volume capture ε_1, due to a valuable fraction of particles, which quickly return from channeling to over-barrier motion (see Fig. 8).

It is useful and interesting to compare our calculation of the total angle curve with the corresponding experimental data. Such data can be found in a number of papers. However, in many cases these data are presented in a linear scale and are statistical insignificant for a comparison for large scattering angles. Nevertheless we could find the article which satisfies our requirements (see Ref. [15]). In the article results are presented for measurements of the total angle curve for 400 GeV protons and silicon plane (110) for ≈18.5 m bending radius and length of crystal along beam equal to 3 mm. These results of measurements are inserted in Fig. 10 as grey lines [the curves 4 and 5, whereas the curve 3 is the Gaussian approximation of the beam divergence and the curve 5 is the measured intensity of protons after the passage through the crystal (in both cases)].

Besides, we think that the correct method of comparison should be based on the comparison normalized on 1 distributions of scattering angles. Also it is desirable to make the comparison for identical parameters of the proton beam. The curve 1 in Fig. 10 presents the result of a calculation for a beam practically without angle divergence. At some likelihood suggestions and knowing the normalized angle distribution $\rho_b(\alpha)$ we can write for the angle distribution function for scattering of the beam:

$$\rho_T(\alpha) = \int_{-\infty}^{\infty} \rho_b(\alpha_1)\rho_c(\alpha_1 - \alpha)d\alpha_1. \qquad (43)$$

In accordance with Ref. [15] we will consider the angle distribution function of the beam as $\rho_b(\alpha) = 1/(\sqrt{2\pi}\sigma_b)\exp -\alpha^2/(2\sigma_b^2)$. For calculations we put $\sigma_b = 8.57$ μrad ([15]). It is interesting that at angles $\alpha \gg \sigma$

we get $\rho_T(\alpha) = \rho_c(\alpha)$. It means that the level of scattering particles depends weakly on the normalized beam angle distribution for large distances.

As was shown in [9,15] the width of the angle orientation range of volume reflection is equal to l_0/R (to a bending angle). The beginning of volume reflection is shifted on the graph of angle scan on value equal to $l_0 R$ from the center of the channeling region (see Fig. 6 in [15], for example). The curves 2 and 3 are calculated for the symmetric case when (in other words) the angle of orientation is shifted on $l_0/(2R)$. The curves 4 and 5 correspond to an orientation angle which is shifted on $\approx l_0/(3R)$ from the channeling region. We give this information for the explanation of the location of channeling peaks in Fig. 10.

In Fig. 10 we see that in the area of scattering angles (0.03—0.07) mrad the experimental intensity of protons (the curve number 4) exceeds the results of our calculations (the curves 2 and 3) approximately by 2 times. However for a correct comparison we should take into account the difference of bending radii (10 m and 18.5 m for calculations and measurement, correspondingly). In our model we can calculate the total normalized number of captured protons ε_1. This calculations with the help of Eq. (42) give $\varepsilon_1 = 0.057$ and 0.105 or the ratio of these values is equal to 1.85. The scattered angle distribution of particles is described with the help of Eqs. (30) and (32). A simple estimation shows that the value $\frac{dN_{de}(\alpha)}{d\alpha}\frac{1}{\epsilon_1}$ is practically independent of the bending radius (at its variations from 5 to 20 m) for crystals with a length about 2–3 mm. Thus we demonstrate that our analytical calculations are in reasonable agreement with the experiment [15] and also with Monte Carlo computations presented in [6].

VI. DISCUSSION

As mentioned above our consideration is valid for small enough bending radii of single crystals. It is clear that for large bending radii the energy gap δE becomes very small. Because of this, the particle energy losses can significantly exceed the value δE, and, consequently, the possibility of volume capture will be realized for a long enough part of the trajectory of particles, instead of the short distance between x_1 and x_3 (see Fig. 1).

Let us estimate the area of application of our analytical description. Taking into account that the distribution of energy losses is described by the normal one, we can write the following condition for the validity of equations obtained in the paper:

$$\sigma_{E,\max} < \delta E/4 \tag{44}$$

where $\sigma_{E,\max}$ is the maximal value of σ_E at fixed κ-parameter. For the (110) silicon plane and proton energy equal to 400 GeV $\delta E/4[eV] \approx 20/R[m]$ and $\sigma_{E,\max} \sim 1$ eV and we got that our consideration is valid up to $R \sim 20$ m (or for $R/R_c \sim 30$). The area of validity is extended with the increasing of the particle energy. It is important to note that the range $R/R_c \approx 10$–20 is preferable for the utilization of the volume reflection process on accelerators. Really, at these values of radii the mean angle α_m of the process is close to the maximal one [2] and the volume capture process is suppressed in comparison with the case of larger bending radii.

In this paper, for small enough bending radii we got a simple relation for the probability of volume capture ε_1 in different single crystals. According to this relation ε_1 is proportional to $E_0^{-\frac{1}{4}}(R/R_c - R_1/R_c)$. It means that ε_1 is a weakly dropping function of the particle energy at fixed R/R_c. For testing this dependence, we carried out Monte Carlo calculations of ε_1 at different radii and energies. The results of these calculations are described by a function which is proportional to $E_0^{-0.2}(R/R_c - 0.7)$. This dependence is close to that obtained in this paper.

The process of volume capture was investigated also in Ref. [11]. Here the probability of volume capture is $\varepsilon_1 = R\theta_{ch}/L_d$, where L_d is the dechanneling length, which is proportional to the particle energy. It means that ε_1 is proportional to $E_0^{-\frac{1}{2}}R/R_c$. The paper [6] contains the criticism of this relation. The authors [6] give the conclusion about the incorrectness of the relation and try to correct it by introducing a nuclear dechanneling length. This correction allows one to get values of probability close to Monte Carlo calculations (for energy 400 GeV) but preserves the previous energy dependence.

In the future we plan to apply our mathematical consideration of volume capture for negative charged particles.

VII. CONCLUSION

The main results of our investigation of volume reflection of relativistic particles are

(i) the analysis of experimental data and the comparison with theoretical calculations of the mean volume reflection angle demonstrate a good mutual agreement;
(ii) simple analytical relations for the probability of volume capture are obtained;
(iii) the propagation of the volume captured fraction inside a single crystal is considered;
(iv) analytical methods for the calculation of the angle scattered distribution of particles, taking into account different processes are developed;
(v) equations presented here allow one to find the efficiency of the volume reflection process but a full analysis of this problem is beyond the scope of this paper.

[1] A. M. Taratin and S. A. Vorobiev, Phys. Lett. A **119**, 425 (1987).
[2] V. A. Maisheev, Phys. Rev. ST Accel. Beams **10**, 084701 (2007).

[3] G. V. Kovalev, JETP Lett. **87**, 349 (2008); **89**, 265 (2009).
[4] M. V. Bondarenco, Phys. Rev. A **82**, 042902 (2010).
[5] N. F. Shul'ga, V. J. Truten, V. V. Boyko, and A. S. Esaulov, Phys. Lett. A **376**, 2617 (2012).
[6] A. M. Taratin and W. Scandale, Nucl. Instrum. Methods Phys. Res., Sect. B **262**, 340 (2007).
[7] Yu. M. Ivanov *et al.*, Phys. Rev. Lett. **97**, 144801 (2006).
[8] Yu. M. Ivanov *et al.*, JETP Lett. **84**, 372 (2006).
[9] W. Scandale *et al.*, Phys. Rev. Lett. **98**, 154801 (2007).
[10] V. A. Andreev *et al.*, *JETP Lett.* ***36****, 415 (1982)*.
[11] V. M. Biryukov, Yu. A. Chesnokov, and V. I. Kotov, *Crystal Channeling and Its Application at High Energy Accelerators* (Springer, New York, 1996).
[12] W. Scandale *et al.*, Phys. Rev. Lett. **101**, 234801 (2008).
[13] W. Scandale *et al.*, Phys. Lett. B **681**, 233 (2009).
[14] S. Bellucci and V. A. MaisheevPhys. Rev. A **86**, 042902 (2012).
[15] W. Scandale *et al.*, Phys. Rev. ST Accel. Beams **11**, 063501 (2008).
[16] R. Rossi, G. Cavoto, D. Mirarchi, S. Redaelli, and W. Scandale, Nucl. Instrum. Methods Phys. Res., Sect. B **355**, 369 (2015).
[17] S. Hasan, Ph.D. thesis, Universitá Degli Studi Dellinsubria, 2011.
[18] W. Scandale *et al.*, Phys. Lett. B **682**, 274 (2009).
[19] Hasan *et al.*, Nucl. Instrum. Methods Phys. Res., Sect. B **269**, 612 (2011).
[20] V. A. Maisheev,Nucl. Instrum. Methods Phys. Res., Sect. B **119**, 42 (1996).
[21] E. Bagli, V. Guidi, and V. A. Maisheev, Phys. Rev. E **81**, 026708 (2010).
[22] W. Scandale *et al.*, Phys. Lett. B **658**, 109 (2008).
[23] D. De Salvador *et al.*, Appl. Phys. Lett. **98**, 234102 (2011).
[24] D. De Salvador *et al.*, J. Appl. Phys. **114**, 154902 (2013).
[25] http://lamp.tu-graz.ac.at/~hadley/ss1/crystaldiffraction/atomicformfactors/formfactors.php.
[26] M. Ter-Mikaelyan, *High Energy Electromagnetic Processes in Condensed Media* (Wiley-Interscience, New York, 1972).
[27] Program for calculation of volume reflection in bent crystals: http://mail.ihep.ru/~maisheev.
[28] L. Bandiera *et al.*, Nucl. Instrum. Methods Phys. Res., Sect. B **309**, 135 (2013).
[29] J. Beringer*et al.*, Phys. Rev. D **86**, 010001 (2012).